


 Cite this: *RSC Adv.*, 2025, **15**, 406

## 3D-printed silicon nitride ceramic implants for clinical applications: the state of the art and prospects

 Peng Zhang<sup>ab</sup> and Rujie He<sup>ab</sup>  <sup>\*b</sup>

$\text{Si}_3\text{N}_4$  ceramic has received great attention because of its sound biological performances, which make it an attractive ceramic implant material in healthcare, particularly in orthopedic surgery. With the advancement of 3D printing technology,  $\text{Si}_3\text{N}_4$  ceramics can now be fabricated into customized implants with precise anatomical shapes, sizes, and microstructures, catering to the individual needs of patients. We, therefore, conducted a comprehensive review of how 3D printing enables complex-shaped  $\text{Si}_3\text{N}_4$  ceramic implants for clinical applications. Firstly, commonly used 3D printing technologies are introduced. Then, the state of the art of the 3D-printed  $\text{Si}_3\text{N}_4$  ceramic implants are summarized. Finally, we forward the prospects towards the 3D printing of  $\text{Si}_3\text{N}_4$  ceramic implants, including high mechanical properties, composites, drug loading, and economics and low cost. We hope that this review will provide a thorough examination and helpful guidance to related scientists, clinicians, and dentists in this field.

Received 9th November 2024

Accepted 18th December 2024

DOI: 10.1039/d4ra07970a

[rsc.li/rsc-advances](http://rsc.li/rsc-advances)

### 1. Introduction

Silicon nitride ( $\text{Si}_3\text{N}_4$ ) is a non-oxide ceramic extensively used in system parts subjected to high stress and/or high temperatures, owing to its outstanding properties such as low density, high strength, high fracture toughness, high hardness, excellent wear resistance and creep behavior, and excellent resistance at elevated temperatures.<sup>1–3</sup> Recently, in addition to its excellent physicochemical and mechanical properties,  $\text{Si}_3\text{N}_4$  ceramic has received great attention because of its sound biological performances, which make it an attractive implant material in healthcare, particularly in orthopedic surgery.<sup>4–6</sup>  $\text{Si}_3\text{N}_4$  ceramic is used clinically in developing bearings in total hip and knee joint replacement, spinal space fusion devices, and so on (as shown in Fig. 1).<sup>7</sup> Some transnational corporations, such as CeramTec Industrial, SINTX Technologies, and so on, have achieved great success in the field of  $\text{Si}_3\text{N}_4$  ceramic hip and knee joint replacement. In addition,  $\text{Si}_3\text{N}_4$  ceramic implants have also been reported to be used in dental clinics. According to some market reports,  $\text{Si}_3\text{N}_4$  ceramic implants will increase at a compound annual growth rate of over 17.5% from 2024 to 2031, perhaps reaching over USD 10 billion. Table 1 lists the possible clinical applications of 3D-printed  $\text{Si}_3\text{N}_4$  ceramic implants, including these dental implants, orthopedic implants, and other customized implants, which show great potential and value.

As is known, ceramic implants are always complex in geometry, sometimes even with porous, gradient, and other shape features. It is a difficult task to manufacture complex-shaped  $\text{Si}_3\text{N}_4$  ceramic components. At present, 3D complex-shaped  $\text{Si}_3\text{N}_4$  ceramic components are commonly produced through two approaches: sintering and machining,<sup>8,9</sup> and near-net forming and sintering.<sup>10,11</sup> Fig. 1 clearly shows the traditionally prepared  $\text{Si}_3\text{N}_4$  ceramic components for all kinds of possible clinical applications. However, for the sintering and machining approach, bulk  $\text{Si}_3\text{N}_4$  ceramic is firstly fabricated by various sintering technologies, such as pressureless sintering, hot pressing, and so on. Complex-shaped  $\text{Si}_3\text{N}_4$  components are subsequently obtained through grinding, turning, and other machining methods. Inevitable defects and damages exist owing to the deadly brittleness and hardness of ceramic during machining, which greatly deteriorate its properties and life.<sup>12–14</sup> In addition, expensive diamond or superalloy machining tools are needed for machining, which greatly increases the costs.<sup>9,12</sup> For the near-net forming and sintering approach, a complex-shaped  $\text{Si}_3\text{N}_4$  green body is usually prepared *via* near-net colloidal processing technologies, such as slip casting, tape casting, injection molding, gel casting, and so on.<sup>11,15,16</sup> After that, the  $\text{Si}_3\text{N}_4$  component is subsequently obtained by using pressureless sintering. However, molds are usually needed, which increase the production cycles and cost. Moreover, extremely complex-shaped  $\text{Si}_3\text{N}_4$  components may contain internal holes or internal surfaces, which are very difficult to achieve. In one word, both these sintering and machining and near-net forming and sintering approaches cannot meet the manufacturing requirement of 3D complex-shaped  $\text{Si}_3\text{N}_4$  ceramic components.

<sup>a</sup>School of Management, Beijing Institute of Technology, Beijing 100081, China

<sup>b</sup>Institute of Advanced Structure Technology, Beijing Institute of Technology, Beijing 100081, China. E-mail: herujie@bit.edu.cn




Fig. 1 Clinical applications of  $\text{Si}_3\text{N}_4$  ceramic components (SINTX Technologies).<sup>7</sup>

Additive manufacturing (AM), also known as 3D printing, is promising for net- and near-net shaping of  $\text{Si}_3\text{N}_4$  ceramic components.<sup>17,18</sup> Recently, many studies have shown that geometrically complex  $\text{SiOC}$ ,<sup>19</sup> oxide,<sup>20</sup> hydroxyapatite,<sup>21</sup>  $\text{SiC}$ ,<sup>22</sup> and ceramic composite<sup>23</sup> components are readily fabricated by 3D printing. Fig. 2 shows published paper numbers with the topics “3D printing” and “ $\text{Si}_3\text{N}_4$ ” to papers with the topic “ $\text{Si}_3\text{N}_4$ ” (Web of Science database from 2014.01 to 2024.11). It is found that, in the past 10 years, the 3D printing of  $\text{Si}_3\text{N}_4$  ceramic has drawn increasing attention and has been subjected to intensive research. Among these studies, an increasing number of novel 3D-printed  $\text{Si}_3\text{N}_4$  ceramic implants have been investigated and used in the biomedical field. However, on the one hand, the state of the art of the 3D printing of  $\text{Si}_3\text{N}_4$  ceramic lacks a comprehensive review and summary. On the other hand, there are still many challenges and issues regarding the 3D printing of  $\text{Si}_3\text{N}_4$  ceramic implants and their biomedical clinic applications, which need to be systematically discussed.

Therefore, this paper aims to systematically review the recent state of the art to assess the prospects for novel 3D-printed  $\text{Si}_3\text{N}_4$

ceramic implants for biomedical applications. The authors hope to provide a deep review and helpful guidance for the related scientists, clinicians, and dentists in this field.

## 2. 3D-printed $\text{Si}_3\text{N}_4$ ceramics

According to the ISO/ASTM 52900:2015—Additive manufacturing,<sup>24</sup> 3D printing technologies can be divided into seven categories: vat photopolymerization (VPP), material extrusion (MEX), material jetting (MJ), binder jetting (BJ), powder bed fusion (PBF), direct energy deposition (DED), and sheet lamination (SL). In this paper, commonly used 3D printing technologies for  $\text{Si}_3\text{N}_4$  ceramics that were published recently are summarized as follows.

### 2.1 Vat photopolymerization (VPP) 3D-printed $\text{Si}_3\text{N}_4$ ceramics

Vat photopolymerization (VPP) 3D printing process is a technique in which photosensitive ceramic slurries are exposed to

Table 1 Possible clinical applications of 3D-printed  $\text{Si}_3\text{N}_4$  ceramic implants

Implants	Description
Dental application	<p>Post-core crown</p> <p>Bone screws, surgical plates, screw shafts, and other devices</p>
Orthopedic application	<p>Hip and knee replacements</p> <p>Cervical spacers and spinal fusion cages</p>
Other clinical applications	<p>3D-printed <math>\text{Si}_3\text{N}_4</math> ceramic implants are promising new implants for restoring large-area dental defects, which can serve as the post portion of a post-and-core crown, providing stable retention force</p> <p>3D-printed <math>\text{Si}_3\text{N}_4</math> ceramic implants can be used as bone screws, surgical plates, screw shafts, and other devices. <math>\text{Si}_3\text{N}_4</math> ceramic can effectively integrate with surrounding tissues and promote new bone formation</p> <p>3D-printed <math>\text{Si}_3\text{N}_4</math> ceramic implants can be used as components for hip and knee replacements. <math>\text{Si}_3\text{N}_4</math> ceramic is an ideal choice for replacing traditional <math>\text{Al}_2\text{O}_3</math> ceramics</p> <p>3D-printed <math>\text{Si}_3\text{N}_4</math> ceramic implants can be used as cervical spacers and spinal fusion cages. Especially in spinal surgery, porous <math>\text{Si}_3\text{N}_4</math> ceramic scaffolds for intervertebral body fusion have achieved remarkable clinical effects</p> <p>3D-printed <math>\text{Si}_3\text{N}_4</math> ceramic implants with precise anatomical shapes, sizes, and microstructures can be applied for other clinical applications</p>



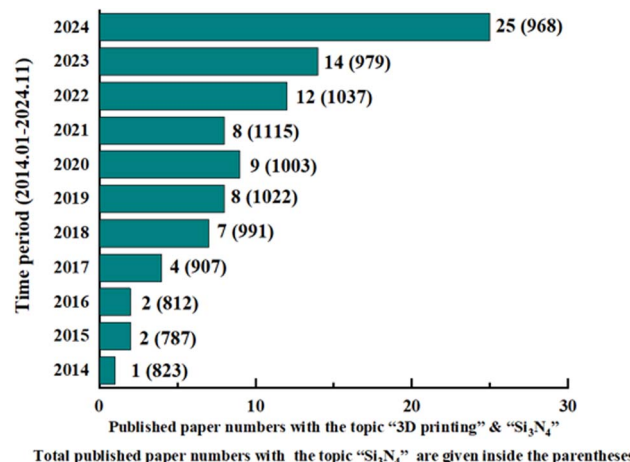


Fig. 2 Published paper numbers with the topics "3D printing" and "Si<sub>3</sub>N<sub>4</sub>" to papers with the topic "Si<sub>3</sub>N<sub>4</sub>" (Web of Science database from 2014.01 to 2024.11).

radiation/light in a controlled manner to obtain polymerized material layers, as shown in Fig. 3a. Subsequent layers combine to form a 3D ceramic green object. After that, debinding and sintering are further conducted to obtain the final ceramic

parts. Usually, VPP 3D printing processes can further be classified into stereolithography (SLA, as shown in Fig. 3a(i)),<sup>25</sup> digital light processing (DLP, as shown in Fig. 3a(ii)),<sup>25</sup> two-photon polymerization (2PP, not shown here),<sup>31</sup> volumetric 3D printing,<sup>32</sup> and so on. Recently, Si<sub>3</sub>N<sub>4</sub> ceramics have been widely reported to be fabricated by VPP 3D printing. Schwarzer-Fischer *et al.* successfully prepared Si<sub>3</sub>N<sub>4</sub> ceramic and its complex structures, such as discs and triple periodic minimal surfaces (TPMS),<sup>33</sup> as shown in Fig. 4a. Zhou *et al.* also fabricated Si<sub>3</sub>N<sub>4</sub> ceramic by VPP 3D printing. Combined with following air pressure liquid-phase sintering, the as-obtained Si<sub>3</sub>N<sub>4</sub> ceramic had a relatively high strength of 382.67 MPa and a density of 2.95 g cm<sup>-3</sup>.<sup>34</sup> They further investigated the effect of thermosetting resin coating modification on the properties of Si<sub>3</sub>N<sub>4</sub> ceramics, as shown in Fig. 4b.

## 2.2 Materials extrusion (MEX) 3D-printed Si<sub>3</sub>N<sub>4</sub> ceramics

Materials extrusion (MEX) 3D printing of ceramics requires continual feeding of material within a moving nozzle. This process enables simple extrusion *via* the nozzle, molding layers along a preset path. After finishing a layer, the build platform or the extrusion head moves up or down, allowing for the deposition and adhesion of another material layer to the previous one. After ceramic green parts are obtained, debinding and

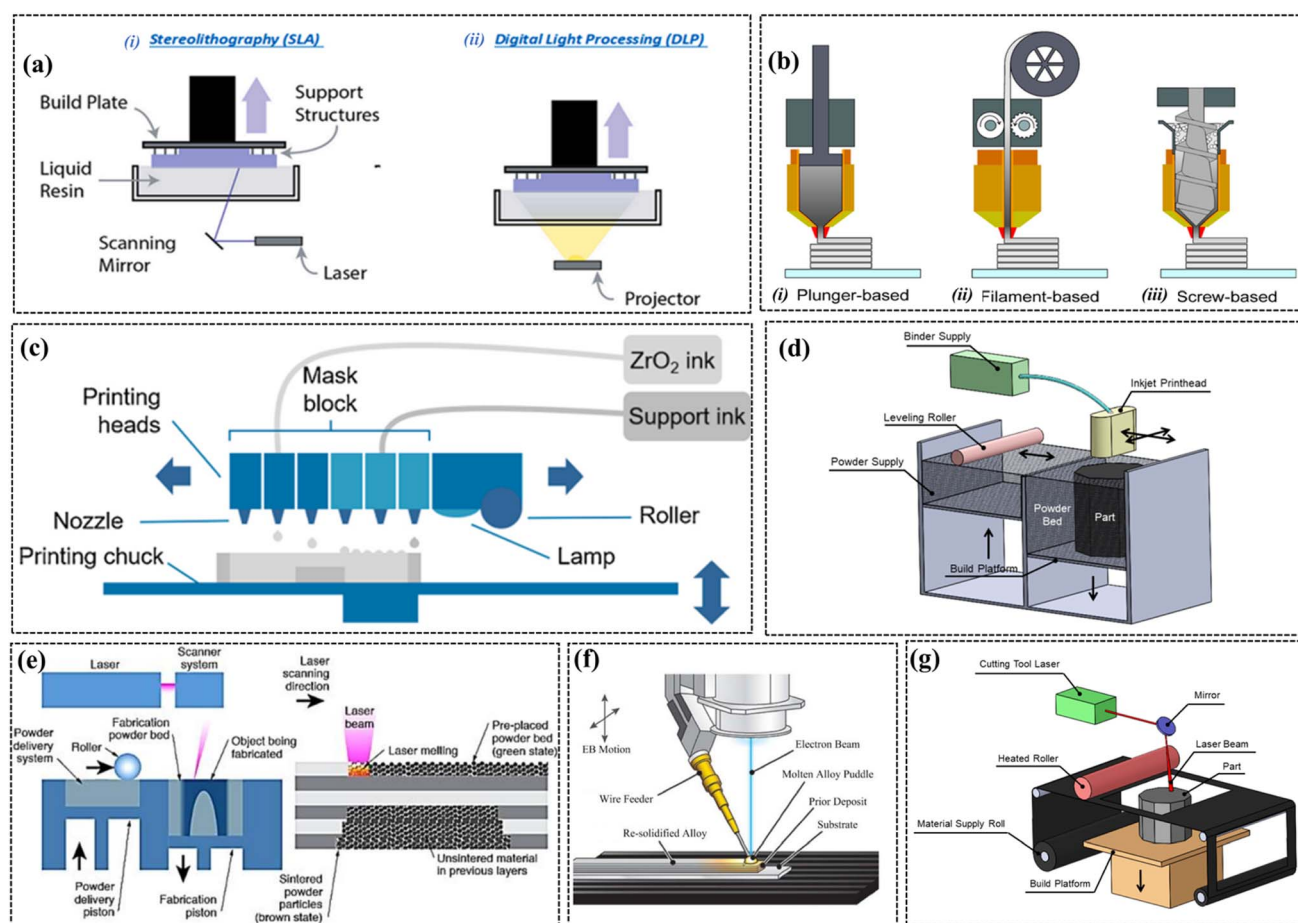


Fig. 3 3D printing technologies: (a) VPP,<sup>25</sup> (b) MEX,<sup>26</sup> (c) MJ,<sup>27</sup> (d) BJ,<sup>28</sup> (e) PBF,<sup>29</sup> (f) DED,<sup>30</sup> and (g) SL.<sup>28</sup>



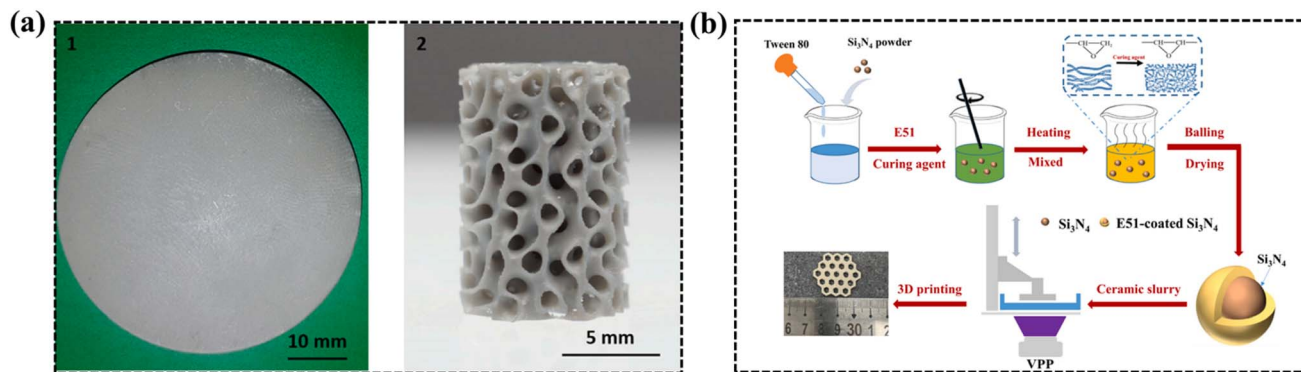


Fig. 4 VPP 3D printing of Si<sub>3</sub>N<sub>4</sub> ceramic: (a) discs and TPMS<sup>33</sup> and (b) thermosetting resin coating modification during 3D printing.<sup>34</sup>

sintering are subsequently conducted. Usually, MEX 3D printing of ceramics can usually be classified into three types (as shown in Fig. 3b): filament-based, plunger-based, and screw-based.<sup>26</sup> Clarkson *et al.* used a UV-assisted direct ink writing (DIW), which is a type of MEX 3D printing, to prepare Si<sub>3</sub>N<sub>4</sub>/SiC from preceramic polymer suspensions.<sup>35</sup> After post-pyrolysis, hexagonal arrays, lattice or log pile structures, and twisted vases were obtained (as shown in Fig. 5a). Jiang *et al.* also prepared Si<sub>2</sub>N<sub>2</sub>O-Si<sub>3</sub>N<sub>4</sub> ceramics *via* DIW and following low-temperature sintering.<sup>36</sup> Spina *et al.* also obtained some Si<sub>3</sub>N<sub>4</sub> ceramic parts, including a rectangular bar, turbine rotor, gear, and swirl fan,<sup>26</sup> by MEX 3D printing, as shown in Fig. 5b.

### 2.3 Material jetting (MJ) 3D-printed Si<sub>3</sub>N<sub>4</sub> ceramics

Material jetting (MJ), also known as direct inkjet printing, is shown in Fig. 3c. This technique makes use of an organic binder to shape the green body component and requires postprocessing such as debinding and sintering to obtain the final densified object.<sup>27</sup> Willems *et al.* attempted to prepare 3Y-TZP ceramic by using MJ 3D printing, with an as-printed green density of 58% and nearly fully sintered density of 6.03 g cm<sup>-3</sup> (99.7% relative density).<sup>27</sup> Complex-shaped ceramic components were successfully achieved by MJ 3D printing, as shown in Fig. 6; however, there has been no report on the MJ 3D printing of Si<sub>3</sub>N<sub>4</sub> ceramic until now.

### 2.4 Binder jetting (BJ) 3D-printed Si<sub>3</sub>N<sub>4</sub> ceramics

Strictly speaking, binder jetting (BJ) 3D printing technology is a type of MJ. Fig. 3d shows the BJ 3D printing of ceramic. The roller spreads the ceramic powder of the powder tank under the nozzle. After that, the nozzle jets the binder to the pre-determined areas. Then, the forming platform descends to a certain height, so back and forth. Finally, a 3D ceramic green body is formed on the forming platform.<sup>28</sup> Rabinskiy *et al.* fabricated porous Si<sub>3</sub>N<sub>4</sub> ceramic using BJ 3D printing technology.<sup>37</sup> Sintered Si<sub>3</sub>N<sub>4</sub> ceramic had a porosity up to 70%. This work provided some ideas for the 3D printing of dense or porous Si<sub>3</sub>N<sub>4</sub> ceramic components.

### 2.5 Powder bed fusion (PBF) 3D-printed Si<sub>3</sub>N<sub>4</sub> ceramics

As shown in Fig. 3e, powder bed fusion (PBF) methods, such as selective laser sintering (SLS), can be employed for 3D printing of ceramics. Normally, ceramic powders are laid on the forming platform. The heat source (laser, plasma, etc.) moves according to the setting path to irradiate the ceramic powders. The temperature of the irradiated ceramic powders hence rises sharply to a temperature lower than the melting point, and sintering occurs. Then, the ceramic powders are spread by a doctor blade and sintered layer by layer, and finally form a 3D complex-shaped ceramic component.<sup>29</sup> Minasyan *et al.* fabricated Si<sub>3</sub>N<sub>4</sub>-based complex geometry parts by SLS.<sup>38</sup> They first

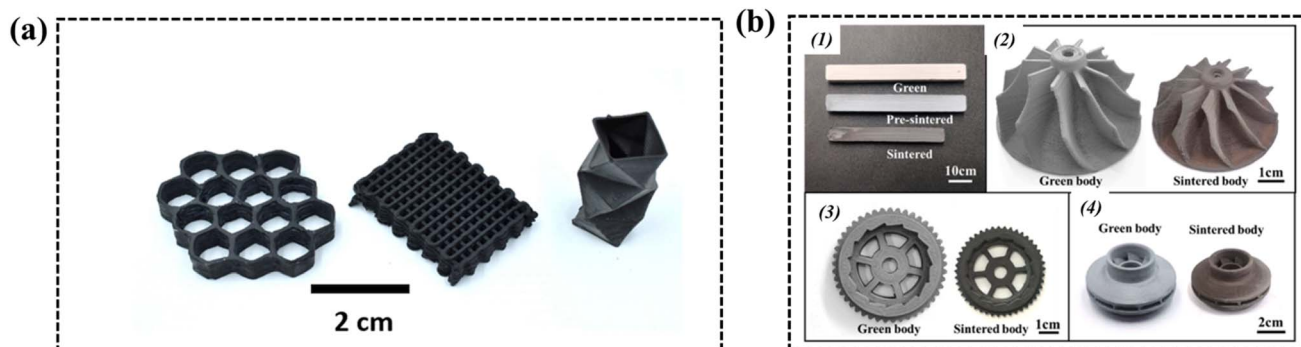


Fig. 5 MEX 3D printing of Si<sub>3</sub>N<sub>4</sub> ceramic: (a) hexagonal array, lattice or log pile structure, and twisted vase;<sup>35</sup> (b) rectangular bar, turbine rotor, gear, and swirl fan.<sup>26</sup>

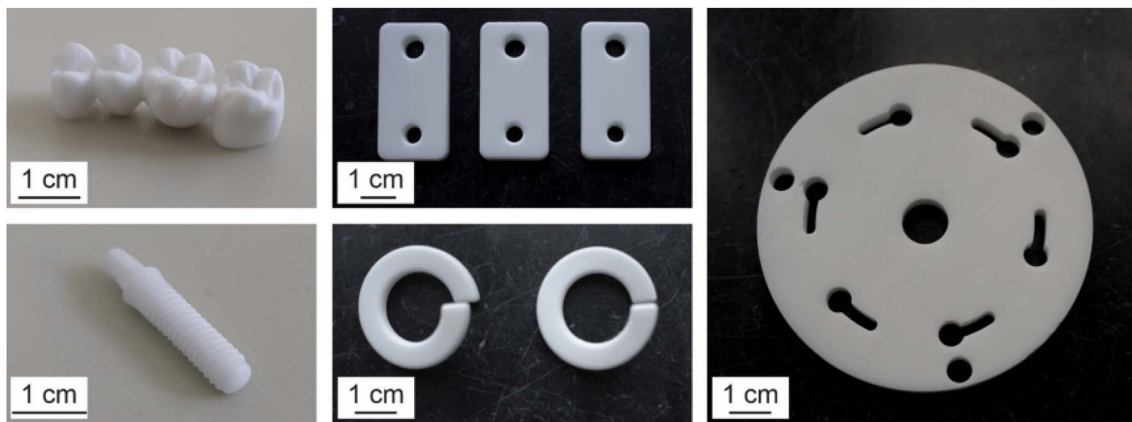


Fig. 6 MJ 3D printing of ceramic components.<sup>27</sup>

used SLS on silicon powder to provide the required shape, and then conducted nitridation on the as-shaped silicon parts to fabricate the  $\text{Si}_3\text{N}_4$  component. Wang *et al.* prepared a high-strength  $\text{Si}_3\text{N}_4$  ceramic antenna window using SLS, combined with cold isostatic pressing (CIP) after debinding before final sintering,<sup>39</sup> as shown in Fig. 7a. The porosity, bulk density, and bending strength of the 3D-printed  $\text{Si}_3\text{N}_4$  ceramic were 18.7%, 3.11 g  $\text{cm}^{-3}$ , and 685 MPa, respectively. Wu *et al.* applied AlN as an inorganic binder during the SLS of porous  $\text{Si}_3\text{N}_4$  ceramic, with a total porosity of 33.6% and a flexural strength of 23.9 MPa, respectively.<sup>40</sup> Finally, they prepared complex-shaped porous  $\text{Si}_3\text{N}_4$  ceramic components, as shown in Fig. 7b.

## 2.6 Direct energy deposition (DED) 3D-printed $\text{Si}_3\text{N}_4$ ceramics

Fig. 3f shows the DED 3D printing.<sup>30</sup> Supply material is directed at the heat source, at the point of deposition. Without the use of hard tooling, this innovative process provides a solution to build complex parts with near-net shapes at a much faster rate than the aforementioned processes. However, there have rarely been any reports on the DED 3D printing of ceramics so far.

## 2.7 Sheet lamination (SL) 3D-printed $\text{Si}_3\text{N}_4$ ceramics

Sheet lamination (SL), also called laminated object manufacturing (LOM), is a 3D printing process in which consecutive layers of paper sheets covered by adhesive applied to one side are continuously bonded and cut with a laser to form a 3D component, as demonstrated in Fig. 3g.<sup>28</sup> Liu *et al.* prepared  $\text{Si}_3\text{N}_4$  ceramic components by aqueous tape casting in

combination with LOM.<sup>41</sup> Homogeneous green  $\text{Si}_3\text{N}_4$  ceramic sheets consisting of 48.7 vol% ceramic particles were prepared by tape casting. Then,  $\text{Si}_3\text{N}_4$  ceramic components with complex shapes were fabricated by layer-by-layer stacking of the green sheets and a subsequent pressureless sintering, as shown in Fig. 8.

To sum up, we summarized the characteristics and advantages/disadvantages of different 3D-printed  $\text{Si}_3\text{N}_4$  ceramics, as listed in Table 2. Each 3D printing technology has its printing accuracy, advantages, and disadvantages. From the comparison between different 3D printing technologies for  $\text{Si}_3\text{N}_4$  ceramics, it is found that VPP and MEX have the most notable accuracy and advantages, resulting in them being widely reported for the preparation of  $\text{Si}_3\text{N}_4$  ceramic implants.

## 3. 3D-printed $\text{Si}_3\text{N}_4$ ceramic implants

Although  $\text{Si}_3\text{N}_4$  ceramic has been widely manufactured by various 3D printing technologies in the past 10 years, the most common 3D-printed  $\text{Si}_3\text{N}_4$  ceramic implants for biomedical applications are mainly obtained by VPP 3D printing and MEX 3D printing.

### 3.1 VPP 3D-printed $\text{Si}_3\text{N}_4$ implants

In 2019, Lithoz GmbH, a famous ceramic 3D printing company, fabricated dense, strong, and precise  $\text{Si}_3\text{N}_4$  ceramic parts by a so-called “lithography-based ceramic manufacturing (LCM)” 3D printing technology, which is a type of VPP 3D printing.<sup>42</sup> They mixed  $\text{Si}_3\text{N}_4$  ceramic particles, solvent, and

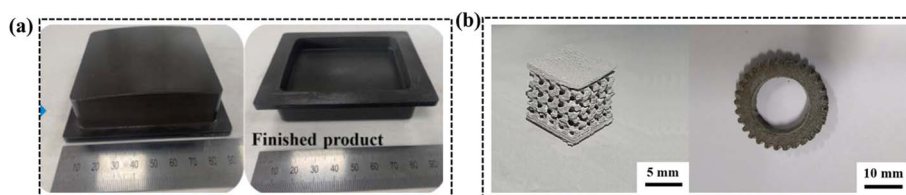


Fig. 7 PBF 3D printing of  $\text{Si}_3\text{N}_4$  ceramic: (a)  $\text{Si}_3\text{N}_4$  ceramic antenna window<sup>39</sup> and (b) complex-shaped porous  $\text{Si}_3\text{N}_4$  ceramic components.<sup>40</sup>

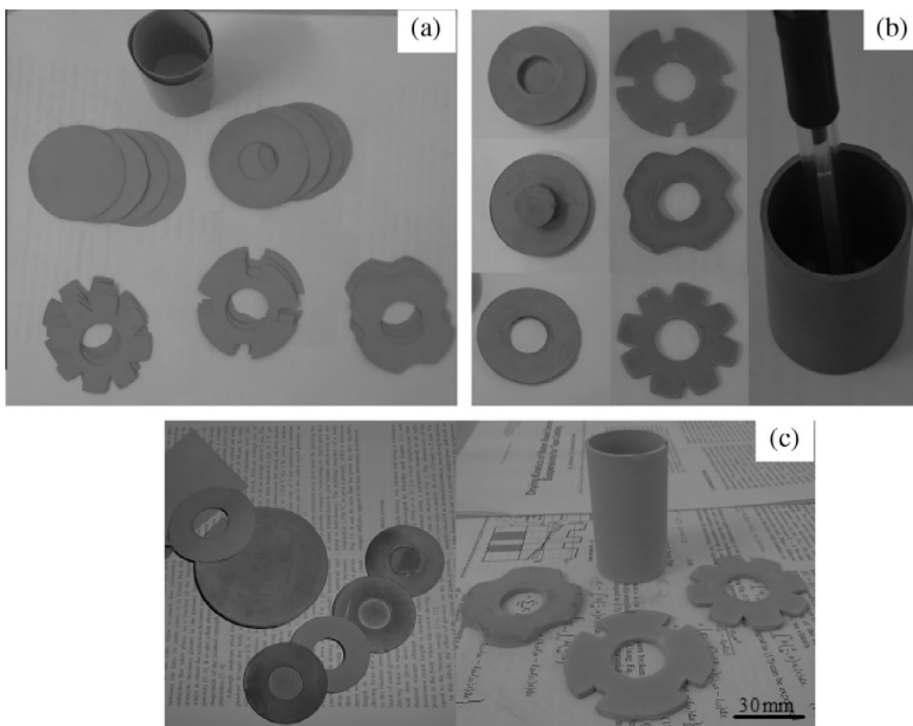


Fig. 8 SL 3D printing of  $\text{Si}_3\text{N}_4$  ceramic: (a) green pieces, (b) green bodies, and (c) sintered components.<sup>41</sup>

a photopolymer network together, and then the as-prepared slurry mixture was cured under 460 nm light.  $\text{Si}_3\text{N}_4$  green parts were 3D-printed, and  $\text{Si}_3\text{N}_4$  final parts were successfully fabricated after debinding and sintering. The LCM 3D-printed  $\text{Si}_3\text{N}_4$  ceramic was reported to have a high relative density (99.8%), high biaxial strength ( $\sigma_f = 764$  MPa), and high hardness ( $\text{HV}_{10} = 1500$ ). They also verified the potential biomedical implant applications, such as dental two-piece implants with M1.6 inner threads, of the LCM 3D-printed  $\text{Si}_3\text{N}_4$  ceramic, as shown in Fig. 9a. After that, many researchers made tremendous efforts in the field of VPP 3D-printed  $\text{Si}_3\text{N}_4$  implants and achieved great progress. In 2023, Zou *et al.* used another kind of VPP 3D printing, digital light processing (DLP), and prepared high-performance VPP 3D-printed  $\text{Si}_3\text{N}_4$  implants for dental use.<sup>43</sup> They first prepared ceramic slurry from  $\text{Si}_3\text{N}_4$  powder, photosensitive resin monomer (HDDA and TMPTA), photo-initiator (Omnirad 380), and sintering additives (yttrium oxide and alumina), with a high solid loading of 40 vol%.  $\text{Si}_3\text{N}_4$  ceramic parts were 3D-printed, debinded, and sintered. The as-

prepared  $\text{Si}_3\text{N}_4$  ceramic has a high three-point flexural strength of 770 MPa and an excellent fracture toughness of  $13.3 \text{ MPa m}^{1/2}$  (as shown in Fig. 9b). They continued to investigate the VPP 3D-printed  $\text{Si}_3\text{N}_4$  implants by *in vitro* biological experiments and found the implants exhibited good biocompatibility. A hemolysis test, oral mucous membrane irritation test, and acute systemic toxicity test (oral route) further confirmed that the VPP 3D-printed  $\text{Si}_3\text{N}_4$  implants did not exhibit hemolysis reaction, oral mucosal stimulation, or systemic toxicity. These findings indicated that VPP 3D-printed  $\text{Si}_3\text{N}_4$  dental implant restorations with personalized structures had good mechanical properties and biocompatibility, which has great application potential in the future.

In addition, porous  $\text{Si}_3\text{N}_4$  ceramic implants were also reported by VPP 3D printing, since porous ceramic structures were beneficial for the following biocompatibility and biomedical applications. In 2023, Huang *et al.* reported a porous  $\text{Si}_3\text{N}_4$  ceramic by VPP 3D printing.<sup>44</sup> They added hawthorn nuclear powder as the pore former and used  $\text{Al}_2\text{O}_3$

Table 2 Comparison between different 3D printing technologies for  $\text{Si}_3\text{N}_4$  ceramics

3D printing	Accuracy	Advantages	Disadvantages
VPP	$\mu\text{m}$	High accuracy	Hard to burn out the resin
MEX	$\mu\text{m-mm}$	Easy forming	Low accuracy, low strength
MJ	$\text{mm}$	—	Low accuracy, low strength
BJ	$\text{mm}$	—	Low accuracy, low strength
PBF	$\mu\text{m-mm}$	—	High thermal stress, high number of defects and cracks
DED	$\mu\text{m-mm}$	—	High thermal stress, high number of defects and cracks
SL	$\text{mm}$	—	Hard to form ceramic sheet

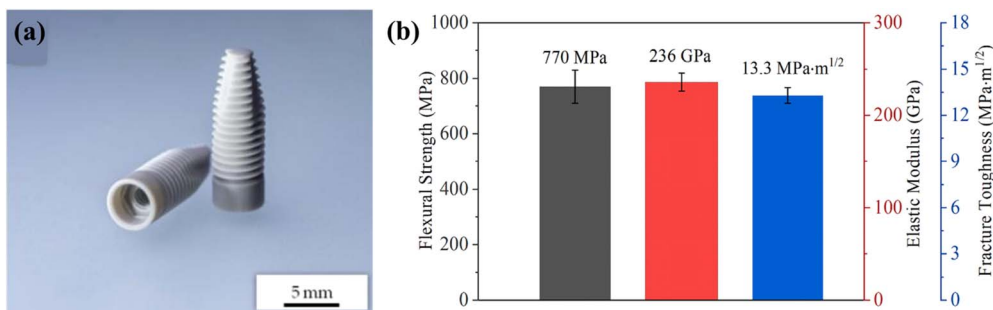


Fig. 9 (a) LCM 3D-printed  $\text{Si}_3\text{N}_4$  ceramic dental two-piece implants;<sup>42</sup> (b) high-performance VPP 3D-printed  $\text{Si}_3\text{N}_4$  implants for dental use.<sup>43</sup>

and  $\text{Y}_2\text{O}_3$  as the sintering additives. The maximum porosity of the VPP 3D-printed  $\text{Si}_3\text{N}_4$  ceramic was 58.48% (as given in Fig. 10a), and the compressive strength and Young's modulus were 79 MPa and 18 GPa, respectively. *In vitro* cytotoxicity assays were performed, and cell viability was assessed. Finally, they 3D-printed porous  $\text{Si}_3\text{N}_4$  ceramic bone for verification (as presented in Fig. 10b and c). The VPP 3D-printed porous  $\text{Si}_3\text{N}_4$  ceramic did not exhibit significant cytotoxicity and was capable of supporting the growth of rat bone marrow mesenchymal stem cells (rBMSC), which indicated excellent biocompatibility and potential for bone application.

### 3.2 MEX 3D-printed $\text{Si}_3\text{N}_4$ implants

In 2016, Zhao *et al.* prepared  $\text{Si}_3\text{N}_4$  ceramic with controlled shape and architecture for biomedical application by using a so-called robocasting technology, which was a kind of materials extrusion 3D printing.<sup>45</sup> In their study, an aqueous paste composed of  $\text{Si}_3\text{N}_4$  powder and sintering additives was prepared with the requisite rheology and formed into structures with different geometry and architecture by using robocasting (as given in Fig. 11a and b). Sintering and hot isostatic pressing

produced an almost fully dense  $\text{Si}_3\text{N}_4$  phase (density = 3.23 g cm<sup>-3</sup>) with a fibrous microstructure. Four-point bending tests of as-fabricated dense  $\text{Si}_3\text{N}_4$  ceramic beams showed a flexural strength of 552 MPa. The as-printed  $\text{Si}_3\text{N}_4$  ceramic parts had a controlled surface roughness, and the average surface roughness ( $R_a$ ) found by AFM was 0.75  $\mu\text{m}$  (as shown in Fig. 11c). They found the  $\text{Si}_3\text{N}_4$  parts fabricated in their study were adequate for orthopedic applications.

In 2020, Sainz *et al.* prepared  $\text{Si}_3\text{N}_4$  ceramic scaffolds intended for bone tissue engineering by direct ink writing (DIW),<sup>46</sup> which was also a kind of MEX 3D printing, as shown in Fig. 12a.  $\text{Si}_3\text{N}_4$  ceramic scaffolds reached densities above 95%, as shown in Fig. 12b and c. The bioactivity of these structures was addressed by evaluating the ion release rate in simulated body fluid. In parallel, atomic force microscopy was used to determine the effect of the filaments surface roughness on protein adsorption (Bovine Serum Albumin) for assessing the potential application of MEX 3D-printed  $\text{Si}_3\text{N}_4$  ceramic scaffolds in bone regeneration.

An improved screw extrusion fused deposition modeling (FDM), which is also a type of MEX 3D printing, was reported to

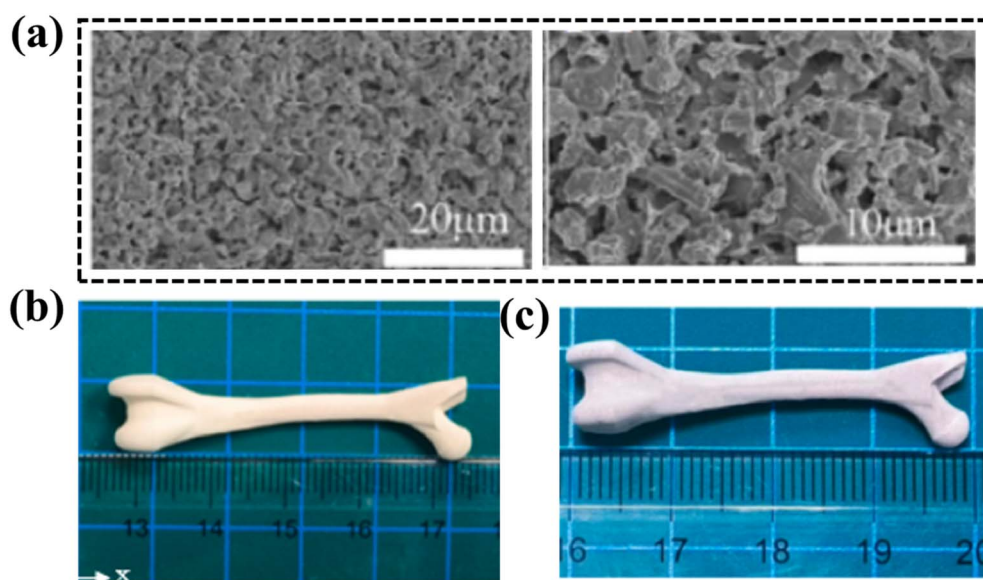


Fig. 10 (a) Porous microstructure, (b) green bone, and (c) sinter bone of VPP 3D-printed porous  $\text{Si}_3\text{N}_4$  ceramic.<sup>44</sup>



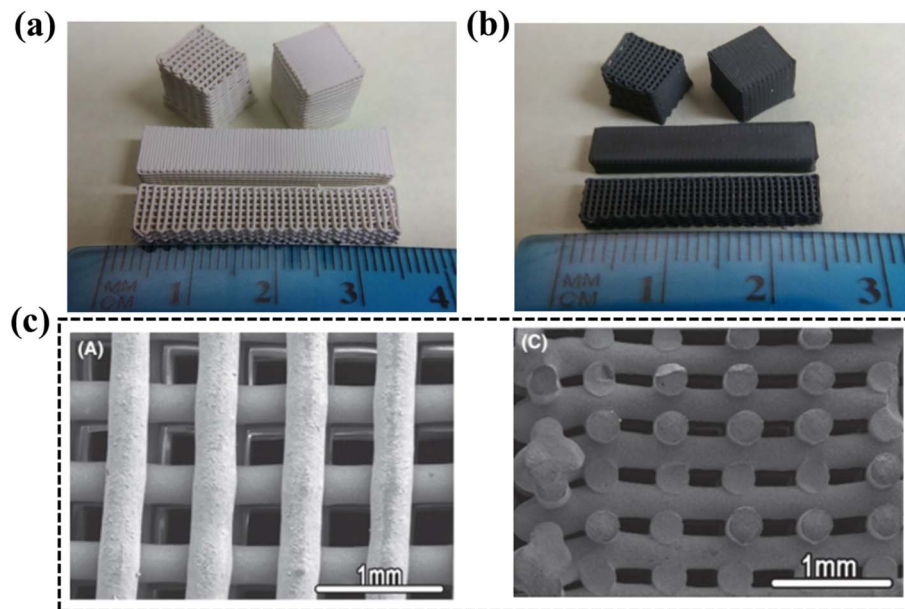


Fig. 11 (a) MEX 3D-printed  $\text{Si}_3\text{N}_4$  ceramic green parts, (b) sintered parts, and (c) microstructures of the architecture.<sup>45</sup>

fabricate  $\text{Si}_3\text{N}_4$  ceramic (as given in Fig. 13a).<sup>47</sup> The authors used 3D printing to achieve customized molding and gas pressure sintering to prepare dense  $\text{Si}_3\text{N}_4$  ceramic and investigated the mechanical properties as well as biological activity. Compared with Ti-alloy,  $\text{Al}_2\text{O}_3$ , and PEEK, 3D-printed  $\text{Si}_3\text{N}_4$  ceramic had significant advantages in mechanical properties with a bending strength of 803 MPa, a fracture toughness of  $8.86 \text{ MPa m}^{1/2}$ , a Vickers hardness of 15.1 GPa, and a compressive strength of 2725 MPa. Meanwhile, the MEX 3D-printed  $\text{Si}_3\text{N}_4$  ceramic had an excellent and more stable biocompatibility compared to biomedical materials and had obvious advantages in antibacterial performance, with an antibacterial rate of 94.6% (as illustrated in Fig. 13b). On the surface of MEX 3D-printed  $\text{Si}_3\text{N}_4$  ceramic, cells had good morphology and normal migration and were more conducive to cell spreading, adhesion, and cross-linking. Their study showed that the melting deposition filling characteristics of the 3D printing method, the crystal-oriented growth microstructure characteristics of 3D-printed  $\text{Si}_3\text{N}_4$  ceramic, and the beneficial effects of silicon and nitrogen elements were the main reasons for achieving these advantages.

In fact, except for the aforementioned 3D printing, other 3D printing technologies, such as SLS, DED, and so on, can also be applied to the 3D printing of  $\text{Si}_3\text{N}_4$  ceramic implants. Indeed, dense or porous  $\text{Si}_3\text{N}_4$  ceramic has been widely reported to be 3D-printed using different technologies.<sup>48–51</sup> We believe that there will be more reports on the  $\text{Si}_3\text{N}_4$  ceramic prepared by different 3D printing technologies and more studies on their microstructure, mechanical properties, biological properties, and real clinical applications.

## 4. Challenges and prospects

Although the 3D printing of  $\text{Si}_3\text{N}_4$  ceramic implants has achieved great developments, there are still many aspects that need to break through in the near future to advance their real clinical applications.

### 4.1 High mechanical properties

Generally, ceramic orthopedic implants need to have excellent mechanical properties, including high mechanical strength,

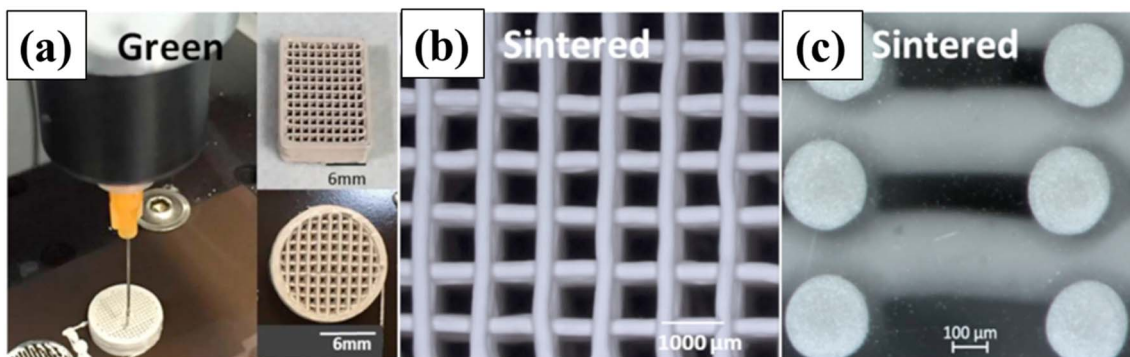


Fig. 12 (a) DIW MEX 3D printing of  $\text{Si}_3\text{N}_4$  ceramic scaffolds and (b and c) microstructures of the green and sintered parts.<sup>46</sup>

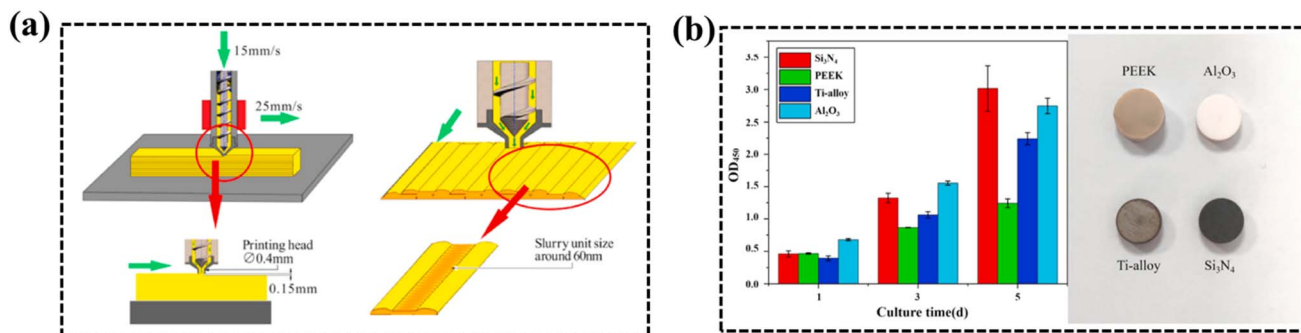


Fig. 13 (a) Improved screw extrusion fused deposition modeling (FDM); (b) excellent biocompatibility of the 3D-printed  $\text{Si}_3\text{N}_4$  ceramic.<sup>47</sup>

high fracture toughness, good fatigue performance, good creep performance, *etc.*

On the one hand, the strength and toughness need to improve. Table 3 lists some of the reported strength and fracture toughness of 3D-printed  $\text{Si}_3\text{N}_4$  ceramic. Fig. 14 further gives the comparison of the relative density and strength of 3D-printed  $\text{Si}_3\text{N}_4$  ceramics by different 3D-printed methods (some relative density or strength data are missing in the references). It is clearly found that most of the 3D-printed  $\text{Si}_3\text{N}_4$  ceramics had a relatively low density, low strength, and low toughness relative to traditional sintered dense  $\text{Si}_3\text{N}_4$  ceramic (usually >99.9% density and >800 MPa strength)<sup>48,49,61</sup> and  $\text{ZrO}_2$  ceramic (usually >99.9% density and even >1000 MPa strength)<sup>62,63</sup> for clinical implant applications. Fortunately, some studies achieved high-performance  $\text{Si}_3\text{N}_4$  ceramic using 3D printing. In order to apply it to real applications in the human body, especially the hips, knee, and dental implants, both high strength and high toughness are needed. Therefore, how to further improve the mechanical properties of materials, especially the strength and toughness, will be the future research focus. On the other hand, in actual human implantation environments, ceramic implants need to withstand fatigue, creep, and other

service environments. Unfortunately, there has been no report about the fatigue and/or creep behavior of 3D-printed  $\text{Si}_3\text{N}_4$  ceramic so far. How to improve the fatigue resistance and creep resistance of 3D-printed  $\text{Si}_3\text{N}_4$  ceramic implants will also be the future focus for applications.

## 4.2 Composites

Compositing ceramic materials with other materials (such as polymers, metals, *etc.*) is another path to achieving high-performance implants. In 2021, Marin *et al.* prepared PMMA/ $\text{Si}_3\text{N}_4$  composites by VPP 3D printing and investigated their antibacterial effects.<sup>64</sup> In 2023, Vidakis *et al.* also prepared polylactic acid/ $\text{Si}_3\text{N}_4$  nanocomposites by MEX 3D printing, and their biodegraded and biomedical behaviors were further discussed.<sup>65</sup> In 2023, Afrouzian *et al.* fabricated  $\text{Si}_3\text{N}_4$ -reinforced  $\text{Ti}_6\text{Al}_4\text{V}$  composites by direct energy deposition (DED) 3D printing technology and studied their bio-tribo-corrosion and antibacterial properties.<sup>66</sup> However, more detailed studies about the 3D-printed composite implants need to be performed.

Moreover, the 3D printing of organic composite implants with ceramics is currently the most promising candidate for bone/chondral repair. Usually, the organics, such as hydrogels

Table 3 Strength and fracture toughness of 3D-printed  $\text{Si}_3\text{N}_4$  ceramics

Material	3D printing	Relative density (%)	Strength (MPa)	Fracture toughness (MPa $\text{m}^{1/2}$ )	Ref.
$\text{Si}_3\text{N}_4$	VPP	99.4	323 <sup>a</sup>	—	52
$\text{Si}_3\text{N}_4$	VPP	88.43	57.3 <sup>b</sup>	—	53
$\text{Si}_3\text{N}_4$	VPP	95	—	5.82	54
$\text{Si}_3\text{N}_4$	VPP	85.4	149.2 <sup>b</sup>	—	55
$\text{Si}_3\text{N}_4$	VPP	95.8	—	6.57	56
$\text{Si}_3\text{N}_4$	VPP	99.8	764 <sup>c</sup>	—	42
$\text{Si}_3\text{N}_4$	VPP	—	770 <sup>b</sup>	13.3	43
Porous $\text{Si}_3\text{N}_4$	VPP	41.52	79 <sup>d</sup>	—	44
$\text{Si}_3\text{N}_4$	MEX	—	552 <sup>b</sup>	—	45
$\text{Si}_3\text{N}_4$	MEX	—	803 <sup>b</sup>	8.86	46
Porous $\text{Si}_3\text{N}_4$	MEX	60–70	53 <sup>b</sup>	—	57
Porous $\text{Si}_3\text{N}_4$	BJ	63.98	47 <sup>b</sup>	—	58
Porous $\text{Si}_3\text{N}_4$	BJ	39	95 <sup>b</sup>	2.4	59
$\text{Si}_3\text{N}_4$	LOM	93.7	475 <sup>b</sup>	—	41
$\text{Si}_3\text{N}_4$	LOM	99.72	725 $\pm$ 26 <sup>b</sup>	7.6 $\pm$ 0.4	60

<sup>a</sup> 3-Point flexural strength. <sup>b</sup> 3-Point flexural strength. <sup>c</sup> Biaxial strength. <sup>d</sup> Compressive strength.

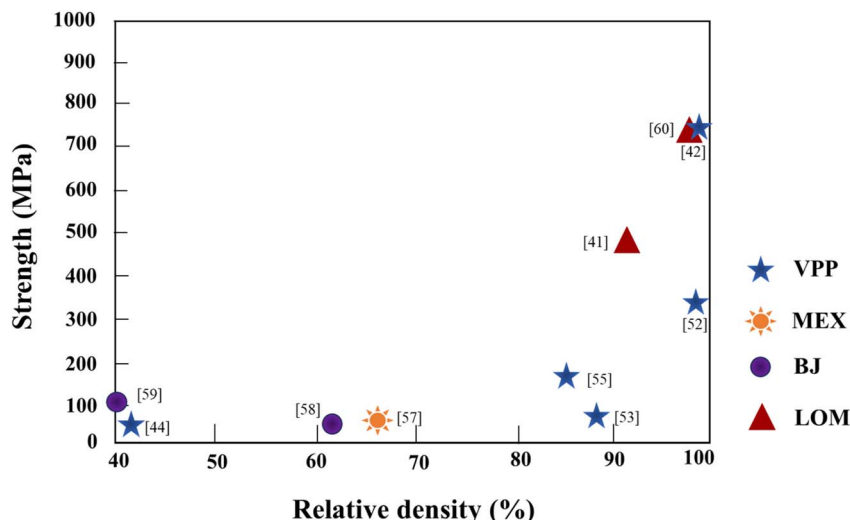


Fig. 14 Comparison of the relative density and strength of 3D-printed  $\text{Si}_3\text{N}_4$  ceramics by different 3D-printed methods (some relative density or strength data are missing in the references).<sup>41,42,44,52–60</sup>

and polymers, provide a cell-like living environment that more closely resembles natural tissue. In the future, *in vitro* and *in vivo* experiments of the 3D-printed bioceramic/organic implants need to be extensively investigated.

#### 4.3 Drug loading

In order to further improve the biocompatibility of the 3D-printed  $\text{Si}_3\text{N}_4$  ceramic implants, loading them with bioactive factors, such as drugs, is an effective approach. Conventional drug therapy often requires systematic administration of higher

doses to achieve the therapeutic dose for the target tissue, resulting in the entire body being affected by side effects. A significant benefit of local drug release is that adequate drug doses can be obtained over a longer period at hard-to-reach sites of action with minimal side effects. Fig. 15 shows the schematic of drug release from the scaffold during bone repair.<sup>67</sup> Drug loading will be an important topic of the 3D-printed  $\text{Si}_3\text{N}_4$  ceramic scaffold implants in future work. It has been demonstrated that biopolymer scaffolds<sup>68,69</sup> and bioceramic scaffolds (hydroxyapatite<sup>70</sup> and tricalcium phosphate<sup>71</sup>) are supportive of

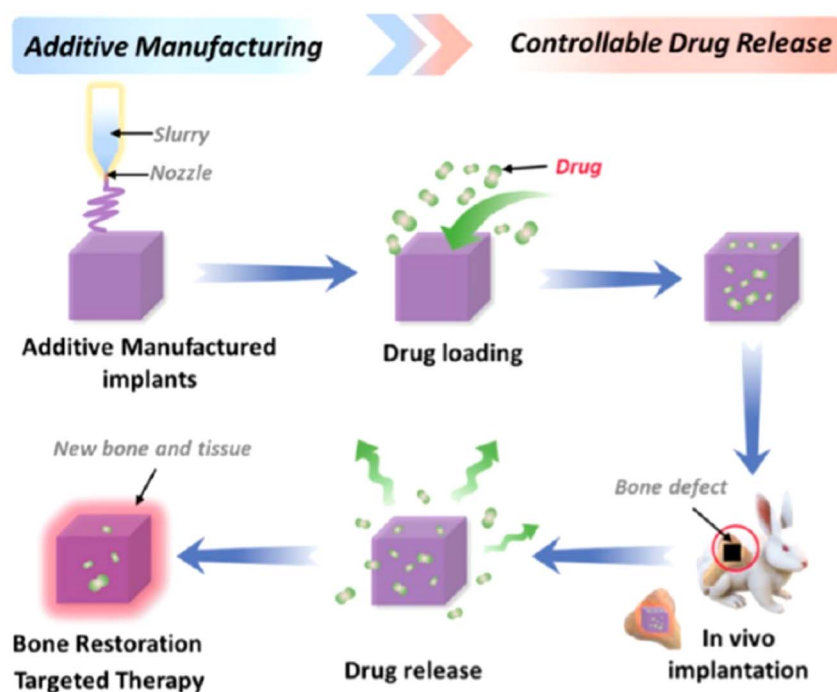


Fig. 15 Schematic representation of drug release from the scaffold during bone restoration.<sup>67</sup>

drug release, which gives a good reference for 3D-printed  $\text{Si}_3\text{N}_4$  implants.

#### 4.4 Economics and low cost

Of course, current implants are basically made of polymers, metals, *etc.* The real clinical application of ceramic implants, especially silicon nitride ceramic implants, still faces the challenge of high costs and high prices. How to reduce the price of medical-grade  $\text{Si}_3\text{N}_4$  powders, how to improve the efficiency and reduce the cost of 3D printing of  $\text{Si}_3\text{N}_4$  ceramic, and how to reduce the cost of biological and clinical evaluation will be the key to the next step in the clinical application of  $\text{Si}_3\text{N}_4$  ceramic implants.

## 5. Conclusions

$\text{Si}_3\text{N}_4$  ceramic is an attractive ceramic implant material in healthcare, particularly in orthopedic surgery. With the advancement of 3D printing technology,  $\text{Si}_3\text{N}_4$  ceramics can now be fabricated into customized implants with precise anatomical shapes, sizes, and microstructures, catering to the individual needs of patients. Therefore, we conducted a comprehensive review of how 3D printing enables complex-shaped  $\text{Si}_3\text{N}_4$  ceramic implants for clinical applications, with the aim of providing helpful guidance for related scientists, clinicians, and dentists in this field. The main conclusions are as follows:

(1) There are seven categories of 3D printing, including VPP, MEX, MJ, BJ, PBF, DED, and SL, that are used to prepare complex-shaped ceramic components. Among them, VPP, MEX, and BJ are the most used 3D printing methods for  $\text{Si}_3\text{N}_4$  ceramic.

(2) The recent state of the art in novel 3D-printed  $\text{Si}_3\text{N}_4$  ceramic implants was summarized. The most common 3D-printed  $\text{Si}_3\text{N}_4$  ceramic implants for biomedical applications are mainly obtained by VPP and MEX 3D printing.

(3) Challenges toward 3D printing of  $\text{Si}_3\text{N}_4$  ceramic implants are discussed. It is clearly found that most of the 3D-printed  $\text{Si}_3\text{N}_4$  ceramic had a relatively low density, low strength, and low toughness compared to traditional sintered dense  $\text{Si}_3\text{N}_4$  ceramic and  $\text{ZrO}_2$  ceramic for clinical implant applications. How to improve the density, strength, toughness, as well as fatigue resistance and creep resistance of 3D-printed  $\text{Si}_3\text{N}_4$  ceramic implants will also be the future focus for applications.

(4) Prospects for the 3D printing of  $\text{Si}_3\text{N}_4$  ceramic implants, such as composites and drug loading, were further analyzed.

## Data availability

All data included in this study are available upon request by contacting the corresponding author.

## Conflicts of interest

There are no conflicts to declare.

## References

- 1 H. Yang and F. Ye, Microtexture, microstructure evolution, and thermal insulation properties of  $\text{Si}_3\text{N}_4$ /silica aerogel composites at high temperatures, *RSC Adv.*, 2022, **12**, 12226–12234.
- 2 J. Zhang, G. Liu, W. Cui, Y. Ge, S. Du, Y. Gao, Y. Zhang, Z. Chen, S. Du and K. Chen, Plastic deformation in silicon nitride ceramics *via* bond switching at coherent interfaces, *Science*, 2022, **378**(6618), 371–376.
- 3 J. Tatami, M. Uda, T. Takahashi, T. Yahagi, M. Iijima, K. Matsui, T. Ohjii and H. Nakano, Microscopic mechanical properties of silicon nitride ceramics corroded in sulfuric acid solution, *J. Eur. Ceram. Soc.*, 2024, **44**(9), 5415–5421.
- 4 R. B. Heimann, Silicon nitride, a close to ideal ceramic material for medical application, *Materials*, 2021, **4**(2), 208–223.
- 5 X. Zeng, C. S. Sipaut, N. M. Ismail, Y. Liu, Y. Y. Farm, B. Feng and J. He, Preparation of 3D printed silicon nitride bioceramics by microwave sintering, *Sci. Rep.*, 2024, **14**, 15825.
- 6 H. Mahammadi, S. Beddu, M. Petrů, M. Sepantař, M. Ebadi, B. K. Yap, L. T. Bang, T. C. Yong, S. Ramesh and S. S. R. Koloor, Advances in silicon nitride ceramic biomaterials for dental applications – A review, *J. Mater. Res. Technol.*, 2024, **28**, 2778–2791.
- 7 SINTX Technologies, available online: accessed on 30 July 2024.
- 8 C. Wu, T. Zhang, W. Guo, X. Meng, Z. Ding and S. Liang, Laser-assisted grinding of silicon nitride ceramics: micro-groove preparation and removal mechanism, *Ceram. Interfaces*, 2022, **48**(21), 32366–32379.
- 9 L. Huang, Y. Dong, Z. Wang, D. Zhang and Z. Yu, Study on the effect of multi-walled carbon nanotube (MWCNT) addition on the microstructure, mechanical and cutting performance of silicon nitride ceramic tools, *Int. J. Refract. Met. Hard Mater.*, 2024, **125**, 106907.
- 10 H. Yang, Z. Wang, M. Sun, F. Chen, J. Ji, S. Chen, Y. Chen, D. Ma, Z. Zhang, B. Pan, Y. Wei and Q. Li, Effect of pH, milling time, and Isobam content on porous silicon nitride ceramics prepared by gel casting, *Adv. Powder Technol.*, 2023, **2**(1), 100060.
- 11 T. G. Aguirre, C. L. Cramer and D. J. Mitchell, Review of additive manufacturing and densification techniques for the net-and near net-shaping of geometrically complex silicon nitride components, *J. Eur. Ceram. Soc.*, 2022, **42**(3), 735–743.
- 12 Y. S. Kwon, J. H. Kim, H. Lee, S. S. Scherrer and H. H. Lee, Strength-limiting damage and defects of dental CAD/CAM full-contour zirconia ceramics, *Dental Mater.*, 2024, **40**(4), 653–663.
- 13 A. Sharama, A. Babbar, Y. Tian, B. P. Pathri, M. Gupta and R. Singh, Machining of ceramic materials: a state-of-the-art review, *Int. J. Interact. Des. Manuf.*, 2022, **17**, 2891–2911.
- 14 Y. Ran, J. Sun, R. Kang, Z. Dong and Y. Bao, Towards understanding the machining process in grinding of



ceramic matrix composites: A review, *Composites, Part B*, 2024, **284**, 111657.

15 S. Yin, W. Wan, X. Fang, H. Ma, X. Xie, C. Zhou, T. Li and R. Zuo, Mechanical and thermal properties of  $\text{Si}_3\text{N}_4$  ceramics prepared by gelcasting using high-solid-loading slurries, *Ceram. Interfaces*, 2023, **49**(24A), 40930–40941.

16 J. Ye, B. Zhang, H. Zhang, Z. Zhong, Y. Wang, Q. Liu and F. Ye, Tuning the dielectric properties of porous BN/ $\text{Si}_3\text{N}_4$  composites by controlling porosity, *J. Eur. Ceram. Soc.*, 2023, **43**(2), 370–377.

17 X. Dong, J. Wu, H. Yu, Q. Zhou, W. Wang, X. Zhang, L. Zhang, L. Li and R. He, Additive manufacturing of silicon nitride ceramics: A review of advances and perspectives, *Int. J. Appl. Ceram. Technol.*, 2022, **19**(6), 2929–2949.

18 Y. Lakhdar, C. Tuck, J. Binner, A. Terry and R. Goodridge, Additive manufacturing of advanced ceramic materials, *Prog. Mater. Sci.*, 2021, **116**, 100736.

19 R. Su, J. Chen, X. Zhang, X. Gao, W. Wang, Y. Li and R. He, Accuracy controlling and mechanical behaviors of precursor-derived ceramic SiOC microlattices by projection micro stereolithography (P $\mu$ SL) 3D printing, *J. Adv. Ceram.*, 2023, **12**(11), 2134–2147.

20 X. Zhai, J. Chen, R. Su, X. Gao, X. Zhang and R. He, Vat photopolymerization 3D printing of  $\text{Al}_2\text{O}_3$  ceramic cores with strip-shaped pores by using polyamide 6 fiber template, *J. Am. Ceram. Soc.*, 2024, **107**(8), 5400–5411.

21 Y. Shan, Y. Bai, S. Yang, Q. Zhou, G. Wang, B. Zhu, Y. Zhou, W. Fang, N. Wen, R. He and L. Zhao, 3D-printed strontium-incorporated  $\beta$ -TCP bioceramic triply periodic minimal surface scaffolds with simultaneous high porosity, enhanced strength, and excellent bioactivity, *J. Adv. Ceram.*, 2023, **12**(9), 1671–1684.

22 W. Wang, Z. Li, X. Gao, Y. Huang and R. He, Material extrusion 3D printing of large-scale SiC honeycomb metastructure for ultra-broadband and high temperature electromagnetic wave absorption, *Addit. Manuf.*, 2024, **85**, 104158.

23 W. Wang, X. Gao, Z. Li, C. Shen and R. He, Effects of ceramic layer height on the mechanical properties of Cf/SiC ceramic matrix composites fabricated by fiber-laying-assisted material extrusion 3D printing, *Compos. Commun.*, 2024, **48**, 101926.

24 ISO/ASTM 52900: 2015-Additive manufacturing, available online: <https://www.iso.org/standard/69669.html>, accessed on 30 July 2024.

25 A. A. Rashid, W. Ahmed, M. Y. Khalid and M. Koç, Vat photopolymerization of polymers and polymer composites: Processes and applications, *Addit. Manuf.*, 2021, **47**, 102279.

26 R. Spina and L. Morfini, Material extrusion additive manufacturing of ceramics: A review on filament-based process, *Materials*, 2024, **17**(11), 2779.

27 E. Willems, M. Turon-Vinas, B. C. dos Santos, B. V. Hooreweder, F. Zhang, B. V. Meerbeek and J. Vleugels, Additive manufacturing of zirconia ceramics by material jetting, *J. Eur. Ceram. Soc.*, 2021, **41**(10), 5292–5306.

28 A. Razavykia, E. Brusa, C. Delprete and R. Yavari, An overview of additive manufacturing technologies—a review to technical synthesis in numerical study of selective laser melting, *Materials*, 2020, **13**(17), 3895.

29 M. S. Korium, H. Roozbahani, M. Alizadeh, S. Perepelkina and H. Handroos, Direct metal laser sintering of precious metals for jewelry applications: process parameter selection and microstructure analysis, *IEEE Access*, 2021, **9**, 126530–126540.

30 A. Selema, M. N. Ibrahim and P. Sergeant, Metal additive manufacturing for electrical machines: Technology review and latest advancements,  *Energies*, 2022, **15**(3), 1076.

31 G. Konstantinou, E. Kakkava, L. Hagelüken, P. V. W. Sasikumar, J. Wang, M. G. Makowska, G. Blugan, N. Nianias, F. Marone, H. V. Swygenhoven, J. Brugger, D. Psaltis and C. Moser, Additive micro-manufacturing of crack-free PDCs by two-photon polymerization of a single, low-shrinkage preceramic resin, *Addit. Manuf.*, 2020, **35**, 101343.

32 M. Regehly, Y. Garmshausen, M. Reuter, N. F. König, E. Israel, D. P. Kelly, C. Y. Chou, K. Koch, B. Asfari and S. Hecht, Xolography for linear volumetric 3D printing, *Nature*, 2020, **588**, 620–624.

33 E. Schwarzer-Fischer, E. Zschippang, W. Kun, C. Koplin, Y. M. Löw, U. Scheithauer and A. Michaelis, CerAMfacturing of silicon nitride by using lithography-based ceramic vat photopolymerization (CerAM VPP), *J. Eur. Ceram. Soc.*, 2023, **43**(2), 321–331.

34 F. L. Zhou, J. M. Wu, C. Tian, W. K. Li, L. Guo, Y. Y. Qin, X. Lin, F. Wang, H. S. Xu and Y. S. Shi, Effect of thermosetting resin coating modification on the properties of  $\text{Si}_3\text{N}_4$  ceramics prepared by vat photopolymerization, *J. Eur. Ceram. Soc.*, 2024, **44**(13), 7465–7473.

35 C. M. Clarkson, C. Wyckoff, M. J. S. Parvulescu, L. M. Rueschhoff and M. B. Dickerson, UV-assisted direct ink writing of  $\text{Si}_3\text{N}_4$ /SiC preceramic polymer suspensions, *J. Eur. Ceram. Soc.*, 2022, **42**(8), 3374–3382.

36 Q. Jiang, D. Yang, H. Yuan, R. Wang, M. Hao, W. Ren, G. Shao, H. Wang, J. Cui and J. Hu, Fabrication and properties of  $\text{Si}_2\text{N}_2\text{O}$ - $\text{Si}_3\text{N}_4$  ceramics via direct ink writing and low-temperature sintering, *Ceram. Int.*, 2022, **48**(1), 32–41.

37 L. Rabinskiy, A. Ripetsky, S. Stinikov, Y. Solyaev and R. Kahramanov, Fabrication of porous silicon nitride ceramics using binder jetting technology, *IOP Conf. Ser.: Mater. Sci. Eng.*, 2006, **140**(1), 012023.

38 T. Minasyan, L. Liu, M. Aghayan, L. Kollo, N. Kamboj, S. Aydinyan and I. Hussainova, A novel approach to fabricate  $\text{Si}_3\text{N}_4$  by selective laser melting, *Ceram. Inter.*, 2018, **44**(12), 13689–13694.

39 K. Wang, C. Bao, C. Zhang, Y. Li, R. Liu, H. Xu, H. Ma, J. Man and S. Song, Preparation of high-strength  $\text{Si}_3\text{N}_4$  antenna window using selective laser sintering, *Ceram. Inter.*, 2022, **47**(22), 31277–31285.

40 Y. R. Wu, J.-H. He, L.-J. Cheng, J.-M. Wu and Y.-S. Shi, Effects of AlN inorganic binder on the properties of porous  $\text{Si}_3\text{N}_4$



ceramics prepared by selective laser sintering, *Ceram. Inter.*, 2022, **48**(20), 29900–29906.

41 S. Liu, F. Ye, L. Liu and Q. Liu, Feasibility of preparing of silicon nitride ceramics components by aqueous tape casting in combination with laminated object manufacturing, *Mater. Design*, 2015, **16**, 331–335.

42 A. A. Altun, T. Prochaska, T. Konegger and M. Schwentenwein, Dense, strong, and precise silicon nitride-based ceramic parts by lithography-based ceramic manufacturing, *Appl. Sci.*, 2020, **10**(3), 996.

43 R. Zou, L. Bi, Y. Huang, Y. Wang, Y. Wang, L. Li, J. Liu, L. Feng, X. Jiang and B. Deng, A biocompatible silicon nitride dental implant material prepared by digital light processing technology, *J. Mech. Behav. Biomed. Mater.*, 2023, **141**, 105756.

44 S. Huang, P. Yang, P. Sheng, T. Ning and S. Wu, Additive manufacturing of complex-shaped and porous silicon nitride-based components for bionic bones, *Ceram. Int.*, 2023, **49**(15), 25025–25034.

45 S. Zhao, W. Xiao, M. N. Rahaman, D. O'Brien, J. W. Seitz-Sampson and B. S. Bal, Robocasting of silicon nitride with controllable shape and architecture for biomedical applications, *Int. J. Appl. Ceram. Technol.*, 2017, **14**(2), 117–127.

46 M. A. Sainz, S. Serena, M. Belmonte, P. Miranzo and M. I. Osendi, Protein adsorption and *in vitro* behavior of additively manufactured 3D-silicon nitride scaffolds intended for bone tissue engineering, *Mater. Sci. Eng. Carbon*, 2020, **115**, 110734.

47 N. Vidakis, M. Petousis, N. Michailidis, V. Papadakis, N. Mountakis, A. Argyros, E. Dimitriou, C. Charou and A. Moutsopoulou, Polylactic acid/silicon nitride biodegradable and biomedical nanocomposites with optimized rheological and thermomechanical response for material extrusion additive manufacturing, *Adv. Biomed. Eng.*, 2023, **6**, 100103.

48 H. Marulcuoglu and F. Kara, Microstructure and mechanical properties of dense  $\text{Si}_3\text{N}_4$  ceramics prepared by direct coagulation casting and cold isostatic pressing, *J. Mater. Sci. Eng. A*, 2022, **854**, 143782.

49 K. Kumar, M. J. Kim, H. M. Oh, Y. J. Park, H. N. Kim, H. J. Ma, J. W. Lee and J. W. Ko, Fabrication of highly dense  $\text{Si}_3\text{N}_4$  via record low-content additive system for low-temperature pressureless sintering, *J. Am. Ceram. Soc.*, 2022, **105**(7), 4669–4680.

50 L. Zhang, W. Ma, Z. Ren, H. Tang, Y. Yu, L. Wang, T. Li, W. Liu and Z. Qiao, Porous  $\text{Si}_3\text{N}_4$  ceramics with surface roughness for bone repair, *Ceram. Int.*, 2024, **50**(5), 7558–7566.

51 N. Kota and S. Roy, Effect of  $\text{H}_3\text{PO}_4$  content and processing temperature on the structure and mechanical properties of porous  $\text{Si}_3\text{N}_4$ , *Ceram. Int.*, 2023, **49**(23), 37174–37186.

52 J. Lüchtenborg, T. Mühler, F. Leonard and J. Günster, Laser-induced slip casting (LIS)-a new additive manufacturing process for dense ceramics demonstrated with  $\text{Si}_3\text{N}_4$ , *J. Ceram. Sci. Technol.*, 2017, **8**(4), 531–540.

53 M. Wang, C. Xie, R. He, G. Ding, K. Zhang, G. Wang and D. Fang, Polymer-derived silicon nitride ceramics by digital light processing based additive manufacturing, *J. Am. Ceram. Soc.*, 2019, **102**(9), 5117–5126.

54 Y. Liu, L. Zhan, Y. He, J. Zhang, J. Hu, L. Cheng, Q. Wu and S. Liu, Stereolithographical fabrication of dense  $\text{Si}_3\text{N}_4$  ceramics by slurry optimization and pressure sintering, *Ceram. Int.*, 2020, **46**(2), 2063–2071.

55 M. Li, H.-L. Huang, J.-M. Wu, Y.-R. Wu, Z.-A. Shi, J.-X. Zhang and Y.-S. Shi, Preparation and properties of  $\text{Si}_3\text{N}_4$  ceramics via digital light processing using  $\text{Si}_3\text{N}_4$  powder coated with  $\text{Al}_2\text{O}_3\text{-Y}_2\text{O}_3$  sintering additives, *Addit. Manuf.*, 2022, **53**, 102713.

56 W.-D. Rao, Y. Liu, L.-J. Cheng and S.-J. Liu, Densification mechanism of stereolithographical dense  $\text{Si}_3\text{N}_4$  ceramics with  $\text{CeO}_2$  as sintering additive by field assisted sintering, *J. Cent. South Univ.*, 2021, **28**(4), 1233–1243.

57 L. N. Rabinskiy, S. A. Sitnikov, V. A. Pogodin, A. A. Ripetskiy and Y. O. Solyaev, Binder jetting of  $\text{Si}_3\text{N}_4$  ceramics with different porosity, *Solid State Phenom.*, 2017, **269**, 37–50.

58 X. Li, L. Zhang and X. Yin, Microstructure and mechanical properties of three porous  $\text{Si}_3\text{N}_4$  ceramics fabricated by different techniques, *Mater. Sci. Eng. A*, 2012, **549**, 43–49.

59 X. Li, L. Zhang and X. Yin, Effect of chemical vapor infiltration of  $\text{Si}_3\text{N}_4$  on the mechanical and dielectric properties of porous  $\text{Si}_3\text{N}_4$  ceramic fabricated by a technique combining 3-D printing and pressureless sintering, *Script Mater.*, 2012, **67**(4), 380–383.

60 F. Niu, X. Yang, Y. Li, J. Guo, P. Liu, Z. Xie and X. Yang, Fused deposition modeling of  $\text{Si}_3\text{N}_4$  ceramics: a cost-effective 3D-printing route for dense and high performance non-oxide ceramic materials, *J. Eur. Ceram. Soc.*, 2022, **42**(15), 7369–7376.

61 L. Fu, H. Engqvist and W. Xia, Spark plasma sintering of biodegradable  $\text{Si}_3\text{N}_4$  bioceramic with Sr, Mg and Si as sintering additives for spinal fusion, *J. Eur. Ceram. Soc.*, 2018, **38**(4), 2110–2119.

62 C. Santos, I. F. Coutinho, J. E. V. Amarante, M. F. R. P. Alves, M. M. Coutinho and C. R. M. Silva, Mechanical properties of ceramic composites based on  $\text{ZrO}_2$  co-stabilized by  $\text{Y}_2\text{O}_3\text{-CeO}_2$  reinforced with  $\text{Al}_2\text{O}_3$  platelets for dental implants, *J. Mech. Behav. Biomed.*, 2021, **116**, 104372.

63 M. Li, S. Cokic, B. V. Meerbeek, J. Vleugels and F. Zhang, Novel zirconia ceramics for dental implant materials, *J. Mater. Sci. Technol.*, 2025, **210**, 97–108.

64 E. Marin, F. Boschetto, M. Zanocco, T. Honma, W. Zhu and G. Pezzotti, Explorative study on the antibacterial effects of 3D-printed PMMA/nitrides composites, *Mater. Design*, 2021, **206**, 109788.

65 N. Vidakis, M. Petousis, N. Michailidis, V. Papadakis, N. Mountakis, A. Argyros, E. Dimitriou, C. Charou and A. Moutsopoulou, Polylactic acid/silicon nitride biodegradable and biomedical Nanocomposites with optimized rheological and thermomechanical response for material extrusion additive manufacturing, *Biomed. Eng. Adv.*, 2023, **6**, 100103.



66 A. Afrouzian and A. Bandyopadhyay, 3D printed silicon nitride, alumina, and hydroxyapatite ceramic reinforced  $Ti_6Al_4V$  composites-Tailored microstructures to enhance bio-tribo-corrosion and antibacterial properties, *J. Mech. Behav. Biomed. Mater.*, 2023, **144**, 105973.

67 Q. Zhou, X. Su, J. Wu, X. Zhang, R. Su, L. Ma, Q. Sun and R. He, Additive manufacturing of bioceramic implants for restoration bone engineering: Technologies, advances, and future perspectives, *ACS Biomater. Sci. Eng.*, 2023, **9**(3), 1164–1189.

68 I. Serris, P. Serris, K. M. Frey and H. Cho, Development of 3D-printed layered PLGA films for drug delivery and evaluation of drug release behaviors, *AAPS PharmSciTech*, 2020, **21**, 256.

69 C. Liu, Z. Wang, X. Wei, B. Chen and Y. Luo, 3D printed hydrogel/PCL core/shell fiber scaffolds with NIR-triggered drug release for cancer therapy and wound healing, *Acta Biomater.*, 2021, **131**, 314–325.

70 S. Chen, Y. Shi, Y. Luo and J. Ma, Layer-by-layer coated porous 3D printed hydroxyapatite composite scaffolds for controlled drug delivery, *Colloids Surf., B*, 2019, **179**, 121–127.

71 J. Yuan, P. Zhen, H. Zhao, K. Chen, X. Li, M. Gao, J. Zhou and X. Ma, The preliminary performance study of the 3D printing of a tricalcium phosphate scaffold for the loading of sustained release anti-tuberculosis drugs, *J. Mater. Sci.*, 2015, **50**, 2138–2147.

